Analysis and Design of a Millimeter-Wave Bandpass Filter with a Stopband in the Specified Higher Frequencies

KAZUYUKI YAMAMOTO, MEMBER, IEEE

Abstract—**The characteristics of a rectangular waveguide bandpass filter (BPF) are not well known in the high-frequency range where higher order modes can propagate. In this paper, the frequency response of a BPF, composed of symmetric inductive windows, is investigated. The range of frequency under investigation covers the region where not only the TE_{10} mode but also higher modes can propagate in the waveguide. A window with incident waves of various modes is first characterized by a scattering matrix. The matrix elements for various modes are obtained in a closed form by means of the variational method. The overall characteristics of the BPF are then obtained by calculating the product of these matrices. A design of a BPF with a stopband in the specified higher frequencies is proposed. Prototype production proved the validity of the theoretical investigation.**

I. Introduction

MANY WORKERS have published investigations concerning the design and characteristics of a rectangular waveguide bandpass filter (BPF) composed of inductive windows and waveguide sections [1]. The previous works are based upon the assumption that only the dominant mode can propagate in the guide. The characteristics of a BPF have not yet been analyzed in the high-frequency range where higher order modes can propagate in the guide. It is desirable that a BPF have one passband only at the design center frequency and have no spurious passbands in other frequency ranges. In this paper, the frequency response of a BPF composed of symmetric inductive windows is investigated up to the frequency range where more than two modes can propagate in the guide. The main problem is to analyze the characteristics of a window with incident waves of higher order modes.

An equivalent circuit of a window with the dominant mode incidence has been studied by several authors [2], [3]. Palais [4] derived the equivalent admittance expression and mode conversion coefficients of an inductive window with the TE_{m0}-mode incidence. However, the equivalent circuit expressed by admittance is not valid for the case where the higher order modes can propagate in the guide. Because the incident higher mode is converted to the lower propagating modes at the window and more than two modes propagate in the guide, a two-port network does not give an accurate expression. In this paper, the equivalent circuit of a BPF with higher mode incident waves is expressed by a scattering matrix. The matrix elements are calculated, based upon the variational principle.

Manuscript received April 21, 1976; revised May 27, 1976.
The author is with the Yokosuka Electrical Communication Laboratory, Nippon Telegraph and Telephone Public Corporation, Yokosuka, Japan.

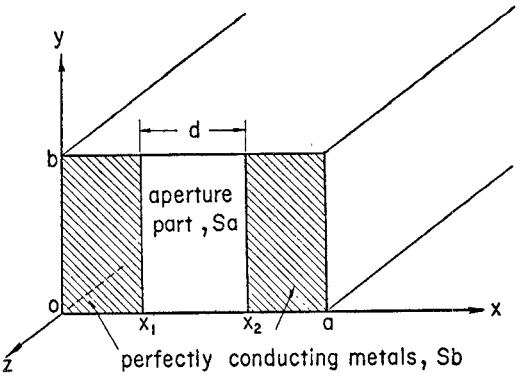

Fig. 1. An inductive window in a rectangular waveguide.

II. Equivalent Circuit of a Window

Formulation of the Problem

A perfectly conducting window with zero thickness is placed in a rectangular waveguide as shown in Fig. 1. In the frequency range where N propagating modes can exist in the guide, the window seen from far away enough is equivalently expressed by a $2N \times 2N$ scattering matrix. Let $a_\alpha^{(I)}$ and $a_\alpha^{(II)}$ $(\alpha = 1, \cdots, N)$ be α-mode incident waves to the window from $z < 0$ and $z > 0$, respectively, and let $b_\alpha^{(I)}$ and $b_\alpha^{(II)}$ be α-mode reflected waves from $z < 0$ and $z > 0$, respectively. The incident waves are related to the reflected waves by the following equation:

$$(b) = (S)(a) \tag{1}$$

where

$$(a) = \begin{pmatrix} a_1^{(I)} \\ \vdots \\ a_N^{(I)} \\ a_1^{(II)} \\ \vdots \\ a_N^{(II)} \end{pmatrix} \quad (b) = \begin{pmatrix} b_1^{(I)} \\ \vdots \\ b_N^{(I)} \\ b_1^{(II)} \\ \vdots \\ b_N^{(II)} \end{pmatrix} \quad (S) = \begin{pmatrix} S_s - E, & S_s \\ S_s, & S_s - E \end{pmatrix} \tag{2}$$

and (E) is an $N \times N$ unit matrix and (S_s) is an $N \times N$ symmetric scattering matrix.

Let us calculate the elements of (S_s). Let a_α and b_β be the electric field amplitude of the incident α mode from $z < 0$ and incident β mode from $z > 0$ to the window, respectively. Then the electric and magnetic fields are expressed by linear combinations of the electric and magnetic mode functions. By applying the mode matching procedure at $z = 0$, we can obtain a variational expression for $S_{\alpha\beta}$, which is the

mode conversion coefficient from α to β mode. $S_{\alpha\beta}$ is expressed as follows:

$$S_{\alpha\beta} = \frac{\sqrt{Y_\alpha Y_\beta}\int_{S_a} \mathcal{E}_\alpha \cdot \boldsymbol{e}_\beta \, dS \int_{S_a} \mathcal{E}_\beta \cdot \boldsymbol{e}_\alpha \, dS}{\sum_{\alpha'} Y_{\alpha'} \int_{S_a} \mathcal{E}_\alpha \cdot \boldsymbol{e}_{\alpha'} \, dS \int_{S_a} \mathcal{E}_\beta \cdot \boldsymbol{e}_{\alpha'} \, dS} \tag{3}$$

where $\boldsymbol{e}_\alpha$, $\boldsymbol{e}_\beta$, and $\boldsymbol{e}_{\alpha'}$ are mode functions of the α-, β-, and α'-mode electric fields, respectively; Y_α, Y_β, and $Y_{\alpha'}$ are α-, β-, and α'-mode characteristic admittances of the guide, respectively; $\mathcal{E}_\alpha$ and $\mathcal{E}_\beta$ are the electric fields at $z = 0$ when only α- and β-mode waves are incident, respectively; and S_a is the aperture as shown in Fig. 1. $S_{\alpha\beta}$ contains unknown functions $\mathcal{E}_\alpha$ and $\mathcal{E}_\beta$. Since (3) is the variational expression for $\mathcal{E}_\alpha$ and $\mathcal{E}_\beta$, we can obtain a more accurate $S_{\alpha\beta}$ from approximate $\mathcal{E}_\alpha$ and $\mathcal{E}_\beta$.

Calculation of the Scattering Matrix

Determination of the scattering matrix is straightforward but requires complicated calculations when many propagating modes are scattered at the window. A more important and relatively simpler case, where only two propagating modes, viz., TE_{11} and TM_{11}, couple each other at a symmetric inductive window, is discussed as an example, other cases can also be solved in this manner.

Let us indicate the TE_{11} and TM_{11} modes by subscripts 1 and 2, respectively. The scattering matrix is expressed by the following form from (2):

$$(S) = \begin{pmatrix} S_{11}-1 & S_{12} & S_{11} & S_{12} \\ S_{12} & S_{22}-1 & S_{12} & S_{22} \\ S_{11} & S_{12} & S_{11}-1 & S_{12} \\ S_{12} & S_{22} & S_{12} & S_{22}-1 \end{pmatrix}. \tag{4}$$

The Rayleigh–Ritz method is applied to (3). Then $\mathcal{E}_1$ and $\mathcal{E}_2$ are expressed by the following trial functions:

$$\mathcal{E}_1 = \sum_{t=1}^{M} C_{1t}\hat{\boldsymbol{e}}_t$$

$$\mathcal{E}_2 = \sum_{t=1}^{M} C_{2t}\hat{\boldsymbol{e}}_t \tag{5}$$

where C_{1t} and C_{2t} are undetermined coefficients; $\hat{\boldsymbol{e}}_t$ is a system of functions which will be chosen in the suitable forms by physical inspections; and M is the number of functions.

Here, we choose $M = 2$, and let $\hat{\boldsymbol{e}}_1$ and $\hat{\boldsymbol{e}}_2$ be similar to the TE_{11}- and TM_{11}-mode electric fields, respectively:

$$\hat{\boldsymbol{e}}_1 = A_{[11]}' f_1(x) \sin\frac{\pi y}{b}\cdot\boldsymbol{a}_x + B_{[11]}' g_1(x)\cos\frac{\pi y}{b}\cdot\boldsymbol{a}_y$$

$$\hat{\boldsymbol{e}}_2 = A_{(11)}' f_2(x) \sin\frac{\pi y}{b}\cdot\boldsymbol{a}_x + B_{(11)}' g_2(x)\cos\frac{\pi y}{b}\cdot\boldsymbol{a}_y$$

$$\frac{dg_1}{dx} = \frac{\pi}{d} f_1 \qquad \frac{dg_2}{dx} = \frac{\pi}{d} f_2 \tag{6}$$

where $\boldsymbol{a}_x$ and $\boldsymbol{a}_y$ are unit vectors in the directions of x and y, respectively, $A_{[11]}'$, $B_{[11]}'$, $A_{(11)}'$, and $B_{(11)}'$ are

$$A_{[mn]}' = \frac{\sqrt{\varepsilon_m\varepsilon_n}\, n}{bK_{mn}'} \qquad B_{[mn]}' = -\frac{\sqrt{\varepsilon_m\varepsilon_n}\, m}{dK_{mn}'}$$

$$A_{(mn)}' = -\frac{2m}{dK_{mn}'} \qquad B_{(mn)}' = -\frac{2n}{bK_{mn}'} \tag{7}$$

and

$$K_{mn}' = \sqrt{m^2\frac{b}{d} + n^2\frac{d}{b}} \qquad \varepsilon_m = \begin{cases} 1, & m = 0 \\ 2, & m \neq 0. \end{cases}$$

TE_{mn} and TM_{mn} modes are indicated by subscripts $[mn]$ and (mn), respectively. The following change in variables [2] is introduced:

$$\cos\frac{\pi x}{a} = \alpha_1 + \alpha_2\cos\theta \tag{8}$$

where α_1 and α_2 are determined so that $\theta = 0, \pi$ at $x = x_1$, x_2. f_1 and f_2 are approximated as follows:

$$f_1(x) = f_2(x) = \cos\theta\cdot\frac{d\theta}{dx}. \tag{9}$$

By substituting (5) into (3) and by means of Rayleigh–Ritz method, we can obtain the matrix elements as follows (see Appendix A):

$$S_{11} = \frac{Y_{[11]}}{\Delta} g_{[11]}{}^{[11]} G_1$$

$$S_{22} = \frac{Y_{(11)}}{\Delta}\left\{ g_{(11)}{}^{(11)} \begin{vmatrix} g_{(11)}{}^{(11)} & G_2 \\ g_{(11)}{}^{[11]} & G_3 + G_4 \end{vmatrix} + g_{(11)}{}^{[11]} \begin{vmatrix} G_1 & g_{(11)}{}^{(11)} \\ G_2 & g_{(11)}{}^{[11]} \end{vmatrix} \right\}$$

$$S_{12} = \frac{\sqrt{Y_{[11]}Y_{(11)}}}{\Delta} g_{[11]}{}^{[11]} \begin{vmatrix} G_1 & g_{(11)}{}^{(11)} \\ G_2 & g_{(11)}{}^{[11]} \end{vmatrix} \tag{10}$$

where G_1, G_2, G_3, G_4, Δ, $g_{[11]}{}^{[11]}$, $g_{(11)}{}^{[11]}$, and $g_{(11)}{}^{(11)}$ are as given in Appendix B.

Thus we have obtained the scattering matrix of a symmetric window with incident TE_{11} and TM_{11} modes in a closed form. It is worth noting that each scattering matrix element is expressed by a rapidly converging series, and that few terms are sufficient for practical computation.

III. Frequency Response of a BPF with Various Incident Modes

The frequency response of a BPF, composed of inductive or capacitive windows with various incident modes, can be analyzed theoretically with the equivalent circuit of a window described in the preceding section. The window and the connecting guide of a BPF are expressed by scattering matrices. Then they are converted into T matrices. By calculating their matrix product, we obtain the overall T matrix, which characterizes the BPF.

The parameters which determine the elements of a scattering matrix are the width of the inductive window,

TABLE I
CUTOFF FREQUENCIES FOR VARIOUS MODES IN THE R-500 WAVEGUIDE

Mode	Cutoff Frequency (GHz)
TE_{10}	31.39
TE_{20}	62.78
TE_{30}	94.18
TE_{01}	62.78
TE_{11}	70.19
TE_{21}	88.79
TM_{11}	70.19
TM_{21}	88.79

TABLE II
EXPRESSIONS FOR THE SCATTERING MATRIX OF A SYMMETRIC INDUCTIVE WINDOW*

Mode	$-\frac{2S_{\alpha\alpha}}{1+S_{\alpha\alpha}}$
TE_{10}	$-j\frac{\lambda_g[10]}{a}\cot^2\left(\frac{\pi d}{2a}\right)$
TE_{20}	$-j\frac{2\lambda_g[20]}{a}\left\{\operatorname{cosec}^4\left(\frac{\pi d}{2a}\right)-1\right\}$
TE_{01}	$j\frac{4a}{\lambda_g[01]}\ln\operatorname{cosec}\left(\frac{\pi d}{2a}\right)$

$$*(S)=\begin{pmatrix} S_{\alpha\alpha}-1 & S_{\alpha\alpha} \\ S_{\alpha\alpha} & S_{\alpha\alpha}-1 \end{pmatrix}$$

waveguide dimension, and frequency. The conditions used in the computation are as follows.

1) The BPF is a four-stage maximally flat direct-coupled type whose center frequency is 43.8 GHz and whose bandwidth is 1.5 GHz.

2) The waveguide used in this BPF is the R-500 (the inside dimension is 4.775 mm × 2.388 mm).

3) The frequency of interest is 40–100 GHz.

4) The window is inductive symmetric with zero thickness.

Table I shows cutoff frequencies of various modes in the R-500 waveguide. It is seen that eight modes can propagate in the band. Among them we choose the TE_{10}, TE_{20}, TE_{01}, TE_{11}, and TM_{11} modes. Two cases are computed: 1) the case where the incident modes are TE_{10}, TE_{20}, and TE_{01}, 2) the case where the incident modes are TE_{11} and TM_{11} and these two modes couple each other. For case 1), a 2 × 2 matrix was used. Expressions for the matrix are shown in Table II. For case 2), the 4 × 4 matrix described in the preceding section was used. Computed frequency responses are shown in Fig. 3 along with the experimental results described below.

The frequency responses of BPF's for various incidents modes were measured by the setup shown in Fig. 2. The output signal of a sweeper goes to a BPF under test through a transformer guide, and the output signal of the BPF is detected by a crystal detector. When we desire the incident mode to be TE_{10} and the scattered modes are all evanescent except TE_{10}, the transformer guide is a taper guide. When we want the incident mode not to be TE_{10} and the scattered modes are all evanescent except the incident mode, the taper guide is replaced by a mode transducer. When the incident mode is converted to other propagating modes at the windows in the BPF, the transformer guide is a mode transducer followed by a mode filter.

The BPF is the four-stage maximally flat type described above, whose center frequency is 43.8 GHz. The measured frequency range is 40–100 GHz. The BPF is made by assembling windows and waveguide sections [5]. The window is constructed by photoetching and the waveguide is constructed by machining.

Experimental results are shown in Fig. 3. Fig. 3(a)–(c) shows the frequency responses for incident TE_{10}, TE_{20}, and TE_{01} modes, respectively, for the frequencies above their cutoff frequencies. Fig. 3(d) shows the results for the TM_{11} mode for 75–100 GHz. Three mode transducers are used. The center frequencies are 75, 85, and 95 GHz and the bandwidth is about 4 percent. When the TM_{11} mode is incident into the BPF, the output modes are TM_{11} and TE_{11}. The output TE_{11} for the incident TM_{11} is the same as the TM_{11} output for the incident TE_{11}, and is shown in Fig. 3(e). Fig. 3(e) shows only theoretical results.

The theoretical and experimental results for each mode are compared below.

(a) TE_{10}: The experimental results agree well with the theoretical ones, as shown in Fig. 3(a). There are passbands at 69 as well as 43.8 GHz. Above 70 GHz, the experimental loss is different from the theoretical one, because the expression for TE_{10} in Table II becomes less accurate in the higher frequencies. Fig. 3(a) shows that above a certain frequency where the TE_{30} mode can propagate (94 GHz in this case), computation by the 2 × 2 matrix becomes inaccurate. Above 94 GHz an accurate scattering matrix expression (described in Section II) is necessary.

(b) TE_{20}: The theoretical computation predicts that there are two narrow dips at 71 and 88.5 GHz; whereas, such dips were not found experimentally. The reason is that the theoretical unloaded Q is higher than the loaded Q in this case; thermal loss masks the resonances obtained by the theoretical computation.

(c) TE_{01}: The experimental results agree well with the theoretical ones below 89 GHz, which is the cutoff frequency of TE_{21} and TM_{21} modes. Above 89 GHz these two modes propagate and, therefore, the accurate scattering matrix representation is necessary.

(d) TM_{11}: Fig. 3(d) shows that the experimental and theoretical results are in good agreement within the bandwidth of mode transducers used in the experiment. Outside these bands imperfections in mode transducing cause ripples in the frequency response.

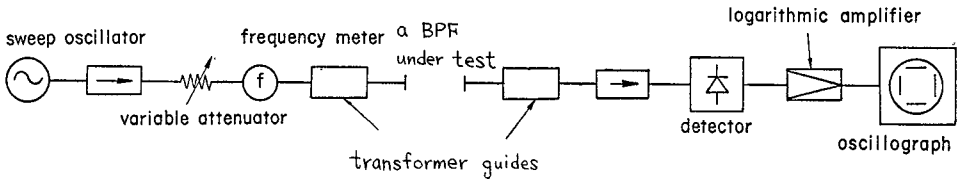

Fig. 2. A setup for measuring the frequency responses of a BPF for various incident modes.

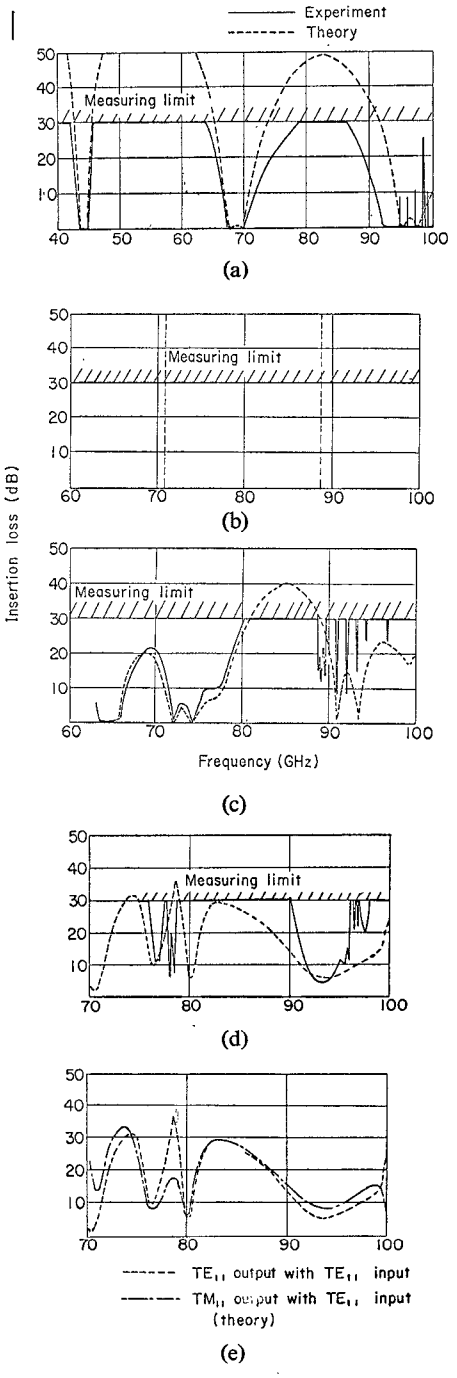

Fig. 3. The frequency responses of the BPF for various incident modes. (a) TE_{10}. (b) TE_{20}. (c) TE_{01}. (d) TM_{11}. (e) TE_{11}.

(e) TE_{11}: It is seen from Fig. 3(e) that for 82–85 GHz the insertion loss is above 25 dB.

From Fig. 3(a)–(e) we find that for 82–85 GHz all TE_{10}, TE_{20}, TE_{01}, TE_{11}, and TM_{11} modes have losses greater than 25 dB. This phenomenon can be used in designing a BPF in which the stopband is located at arbitrary frequencies.

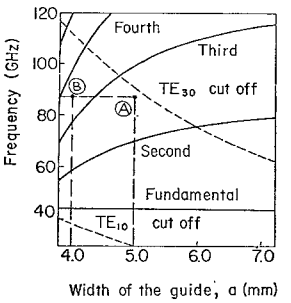

Fig. 4. Higher order resonant frequencies of BPF's for the incident TE_{10} mode.

IV. Design and Production of a BPF with a Stopband in a Specified Higher Frequency Range

The design of a BPF with a stopband around a certain specified frequency is described. We consider the case where the BPF is composed of symmetric inductive windows and rectangular waveguide sections. A frequency range between two cutoff frequencies of TE_{10} and TE_{30} is considered. The outline of design is as follows.

First, in order to reduce the number of modes which can propagate in the waveguide, the height of waveguide is reduced compared with the standard size. Next, the width of waveguide and the apertures and positions of the windows are found by computation of various combinations of these three parameters; in this case, the passband should be kept unchanged.

Let us determine the dimensions of a four-stage maximally flat BPF whose center frequency is 43.8 GHz and whose 3-dB bandwidth is 1.5 GHz. We require the BPF to have a stopband around 88 GHz. The waveguide size is R-500. First, we reduce the waveguide height to less than 1.7 mm. When the height is 1.7 mm, the cutoff frequency of the TE_{01} mode is 88 GHz. Next, the waveguide width and the apertures and positions of the windows should be determined. BPF's with various combinations of waveguide width and apertures and positions of the windows are made for the given center frequency, 3-dB bandwidth, and four-stage maximally flat type [1]. The frequency response of each BPF is computed in the manner described in Section III. The computed curves show that there are several passbands for each BPF. Fig. 4 shows the cutoff frequencies of TE_{10} and TE_{30} modes, and the center

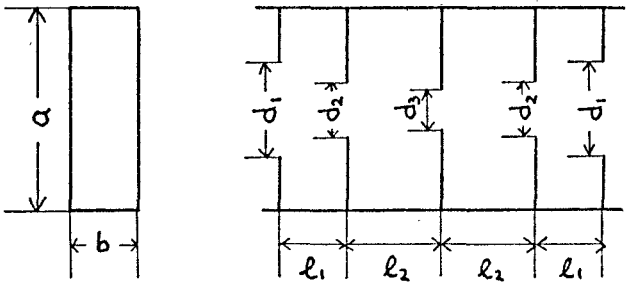

Fig. 5. The structure of the BPF designed with a stopband around 87.6 GHz. Dimensions in millimeters: $a = 4.90$, $b = 1.62$, $d_1 = 2.26$, $d_2 = 1.23$, $d_3 = 1.01$, $l_1 = 3.98$, $l_2 = 4.42$.

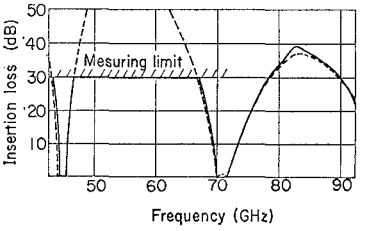

Fig. 6. The frequency response of the BPF for the incident TE_{10} mode.

frequency of the passband of this BPF as a function of the waveguide width. In this figure the apertures and positions of the windows are chosen so as to give the same center frequency and 3-dB bandwidth. The broken lines show TE_{10} and TE_{30} cutoff frequencies. The solid lines show the center frequency of the passband. The passbands spread ± 1 GHz around those curves. The region surrounded by those curves is made up of stopbands. Let us determine the waveguide width for which 1) the TE_{10} and TE_{30} modes are cut off at 88 GHz, and 2) the TE_{10} mode passes through at 43.8 GHz. We find that regions A and B satisfy the above conditions. The waveguide width should be chosen to be 4 or 5 mm. Since region B is very close to the TE_{10} cutoff and the stopband is narrower, region A is more appropriate for our purpose. In region A, only TE_{10} and TE_{20} modes can propagate in the waveguide and the other TE and TM modes are all evanescent.

Fig. 5 shows the structure of the BPF used in the experiment. Fig. 6 shows the frequency response of the BPF. The solid line shows the experimental results and the dotted line shows the theoretical results. It was pointed out in Section III that the computation of the frequency response for the incident TE_{10} mode becomes less accurate in the higher frequencies because the expression in Table II becomes less accurate. Therefore, the following more accurate expression [2] is used here:

$$-\frac{2S_{\alpha\alpha}}{1+S_{\alpha\alpha}} = \frac{2\pi}{a\gamma_{[10]}}\cot^2\left(\frac{\pi d}{2a}\right) \cdot \left\{1 + \frac{3\left(\gamma_{[30]} - \frac{3\pi}{a}\right)\sin^2\left(\frac{\pi d}{2a}\right)\cos^2\left(\frac{\pi d}{2a}\right)}{\frac{3\pi}{a} + \left(\gamma_{[30]} - \frac{3\pi}{a}\right)\sin^6\left(\frac{\pi d}{2a}\right)}\right\}. \tag{11}$$

The experimental result agrees well with the theoretical one for the 40–92-GHz range.

V. Conclusion

In this paper, the equivalent circuit of a BPF is expressed by a scattering matrix, and the procedure for calculating the matrix element by means of the variational principle is given. As an example, an important but relatively simpler case, where TE_{11} and TM_{11} are incident into a symmetric window, is calculated. Then the frequency responses of the BPF, composed of symmetric inductive windows and rectangular waveguide sections, are computed for various incident modes and compared with the experimental results. It has been confirmed that the frequency responses of a BPF are well explained theoretically. Finally, a design of a BPF with a stopband in the specified higher frequency region was outlined. The prototype BPF's were produced in the millimeter-wave region and the expected results were achieved.

The description of this paper is limited to a BPF composed of symmetric inductive windows in the frequencies where relatively lower order modes propagate. This analysis can, however, be applied to other types of BPF's such as filters composed of capacitive windows or asymmetric windows. The analysis can be also applied to the frequency range where other higher order modes can propagate.

Appendix A
Derivation of (10)

If (5) is substituted into (3), and (3) is partially differentiated with respect to C_{1t}, simultaneous equations for C_{2t} are obtained. The condition that they do not have trivial solutions is

$$\det\left(\frac{\sqrt{Y_\alpha Y_\beta}}{S_{\alpha\beta}} g_\alpha^{\,i} g_\beta^{\,j} - \sum_{\alpha'} Y_{\alpha'} g_{\alpha'}^{\,i} g_{\alpha'}^{\,j}\right) = 0, \qquad i,j,\alpha,\beta = 1,2 \tag{A-1}$$

where

$$g_\alpha^{\,i} = \int_{S_a} \hat{e}_i \cdot e_\alpha \, dS. \tag{A-2}$$

The mode function of the TM_{pq} mode electric field is given as follows [3]:

$$e_{(pq)} = A_{(pq)} \cos\frac{p\pi x}{a} \sin\frac{q\pi y}{b} \cdot a_x + B_{(pq)} \sin\frac{p\pi x}{a} \cos\frac{q\pi y}{b} \cdot a_y \tag{A-3}$$

where

$$A_{(pq)} = -\frac{2p}{aK_{pq}} \qquad B_{(pq)} = -\frac{2q}{bK_{pq}}$$

$$K_{pq} = \sqrt{p^2\frac{b}{a} + q^2\frac{a}{b}}. \tag{A-4}$$

Partial integration is carried out over the whole aperture of the window. Here we impose the boundary conditions upon $\hat{e}_i$ at the window. Then we obtain the following equation:

$$\int_{S_a} \hat{e}_2 \cdot e_{(pq)}\, dS = \frac{b}{2}\left(A_{(p1)}A_{(11)}' + \frac{a}{pd}B_{(p1)}B_{(11)}'\right)\int_{x_1}^{x_2} f_2(x)\cos\frac{p\pi x}{a}\,dx. \tag{A-5}$$

The characteristic admittance of the TM_{mn} mode is

$$Y_{(pq)} = \frac{j\omega\varepsilon}{\gamma_{pq}} \tag{A-6}$$

where γ_{pq} is the propagation constant of the TM_{mn} mode. From (7)–(9), (A-5), and (A-6),

$$\sum_{p,q} Y_{(pq)}\left[\int_{S_a}\hat{e}_2\cdot e_{(pq)}\,dS\right]^2 = j\omega\varepsilon\frac{4b^2}{K_{11}'^2d^2}\int_0^{\pi}\int d\theta\, d\theta' \cos\theta\cos\theta' \cdot\left[\frac{1}{\pi b}\left\{-\frac{1}{2}\ln\alpha_2 + \sum_{p=1}^{\infty}\frac{1}{p}\cos(p\theta)\cos(p\theta')\right\} + \sum_{p=1}^{\infty}\left(\frac{K_{p1}^2}{\gamma_{p1}p^2b^2} - \frac{1}{\pi pb}\right)\cdot\sum_{l=0}^{p}\sum_{s=0}^{p}Q_{pl}Q_{ps}\cos(l\theta)\cos(s\theta')\right] \tag{A-7}$$

where Q_{p1} is defined as follows:

$$\cos\frac{p\pi x}{a} = \sum_{l=0}^{p} Q_{pl}\cos(l\theta). \tag{A-8}$$

Integration of (A-7) is carried out, the other terms in (A-1) are calculated in the same way, and we obtain (10).

Q.E.D.

Appendix B
Expressions for Terms in (10)

$$g_{[11]}^{[11]} = \frac{\pi\alpha_2 K_{11}'}{K_{11}d} \qquad g_{(11)}^{(11)} = \frac{\pi\alpha_2 K_{11}}{K_{11}'d}$$

$$g_{(11)}^{[11]} = \frac{\pi\alpha_2}{K_{11}K_{11}'}\left(-\frac{1}{a} + \frac{a}{d^2}\right)$$

$$G_1 = \frac{j\omega\varepsilon\pi^2b^2}{K_{11}'^2d^2}\left[\frac{1}{\pi b} + \sum_{t=1,3,5,\cdots}\left(\frac{K_{t1}^2}{\gamma_{t1}t^2b^2} - \frac{1}{\pi tb}\right)Q_{t1}^2\right]$$

$$G_2 = \frac{j\omega\varepsilon\pi^2 b}{K_{11}'^2 d}\left[-\frac{1}{\pi b} - \sum_{t=1'3'5'\cdots}\cdot\left\{\frac{1}{\gamma_{t1}tb}\left(\frac{t}{a} - \frac{a}{td^2}\right) - \frac{1}{\pi td}\right\}\right]Q_{t1}^2$$

$$G_3 = \frac{\pi^2K_{11}'^2}{j\omega\mu d^2}\left[\frac{\pi}{b} + \sum_{t=1,3,5,\cdots}\left(\frac{\gamma_{t1}}{K_{t1}^2} - \frac{\pi}{tb}\right)Q_{t1}^2\right]$$

$$G_4 = \frac{j\omega\varepsilon\pi^2}{K_{11}'^2}\left[\frac{1}{\pi b} + \sum_{t=1,3,5,\cdots}\cdot\left\{\frac{1}{\gamma_{t1}K_{t1}^2}\left(\frac{t}{a} - \frac{a}{td^2}\right)^2 - \frac{1}{\pi tb}\right\}\right]Q_{t1}^2$$

$$\Delta = \begin{vmatrix} G_1 & G_2 \\ G_2 & G_3 + G_4 \end{vmatrix}. \tag{A-9}$$

Acknowledgment

The author thanks Dr. K. Miyauchi, Dr. S. Shimada, Dr. M. Akaike, and N. Kanmuri for their encouraging discussions, and K. Tachibana and M. Nakayama for their help in the numerical computations and experiments. Thanks are also extended to Fujitsu Laboratory Ltd. and Nippon Electric Company Ltd. for their help in manufacturing BPF's.

References

[1] G. L. Matthaei *et al.*, *Microwave Filters, Impedance-Matching Networks, and Coupling Structures.* New York: McGraw-Hill, 1964.
[2] L. Lewin, *Advanced Theory of Waveguides.* London, England: Iliffe & Sons, Ltd., 1951.
[3] N. Marcuvitz, *Waveguide Handbook.* New York: McGraw-Hill, 1951.
[4] J. C. Palais, "A complete solution of the inductive iris with TE_{ko} incidence in rectangular waveguide," *IEEE Trans. Microwave Theory Tech.*, vol. MTT-15, pp. 156–160, March 1967.
[5] T. Nakagami *et al.*, "Rectangular waveguide band-pass filter for millimeter-waves," *Trans. IECE of Japan*, vol. 55-B, no. 12, pp. 699–701, Dec. 1972.